International Journal of the Physical Sciences Vol. 6(6), pp. 1267-1282, 18 March, 2011
Available online at http://www.academicjournals.org/IJPS
DOI: 10.5897/IJPS10.600
ISSN 1992 - 1950 ©2011 Academic Journals

Full Length Research Paper

3-D numerical analysis of orthogonal cutting process via mesh-free method

Eyup Bagci

TÜBiTAK-UME, National Metrology Institute, P. K. 54, 41470, Gebze-Kocaeli, Turkey. E-mail: eyup_bagci@yahoo.com.

Accepted 22 December, 2010

In this paper, the applications of mesh-free SPH (Smoothed Particle Hydrodynamics) methodology to the simulation and analysis of 3-D hard machining process is presented. A Langrangian SPH based model is carried out using the Ls-Dyna software. Classical Lagrangian, Eulerian and ALE methods such as finite element methods (FEM) cannot resolve the large distortions very well. Conventional finite element analysis of metal cutting processes often breaks down due to severe mesh distortion. Recent developments in so called mesh-free or meshless methods provide alternates for traditional numerical methods in modeling the machining processes. SPH is a mesh-free approach, so large material deformations that happen in the analysis of cutting problem are easily managed and SPH contact control permits an "inherent" chip/workpiece separation. Because SPH combines the advantages of mesh-free, langrangian, particle methods, an alternative methodology, which appears to eliminate most of those difficulties is that of meshless methods. The orthogonal cutting process of AISI H13 steel material was modeled and analysed using SPH method. The developed SPH model gained its ability to correctly estimate the cutting forces, as illustrated in two orthogonal cutting situations. Cutting forces were compared for SPH, Langrangian explicit and experimental results. The predicted (SPH) cutting forces agree within 8.43% and 11.70% of the measured values for tangential and normal components respectively. A good agreement between predicted and experimental cutting forces was observed.

Key words: Machining, cutting, mesh-free methods, meshless, SPH, Eulerian, ALE, Langrangian

INTRODUCTION

Metal cutting plays a very important role in mechanical manufacturing area, the nature of machining being concerned with many related subjects of technology and industry. In the machining processes, material is removed from the surface of the work-part by a cutter and a chip is formed. The complexities are due to large deformation and high strain-rate in the primary shear zone and due to the frictional contact between the cutter and chip along the secondary shear zone. Experiments, which have been used to study metal machining, are very expensive and time consuming. Alternative approaches are computational methods, boundary element, finite difference and finite element methods, analytical methods are the most popular.

Orthogonal metal cutting problems include passing a relatively hard cutter through a softer work-part, and this process is properly simulated by solving the nonlinear governing equations in a zone very near the cutter as shown in Figure 1. Analytical approaches of orthogonal metal cutting were first considered by Ersnt and Merchant (1941), who introduced the concept of the shear angle, and classic theory such as slip lines, Lee and Shaffer (1951) have been used in the past the explore the cutting and to estimate cutting forces. Although these methods need some kinematics assumptions and are somewhat limited to simplified material (constitutive material model equations) response, all these analytical models provided a useful insight to the cutting process. In the 1970s, Klamecki (1973); Okushima and Kakino (1971); and Tay and Stevenson (1974) pioneered the use of finite element (FE) approach to analyze and simulate the orthogonal cuting. The main advantage of using FEA compared to other empirical and analytical approaches is its capability to represent workpiece and cutting tools material properties as a function of strain rate, temperature, friction coefficient, stress, strain, ductile and brittle damage

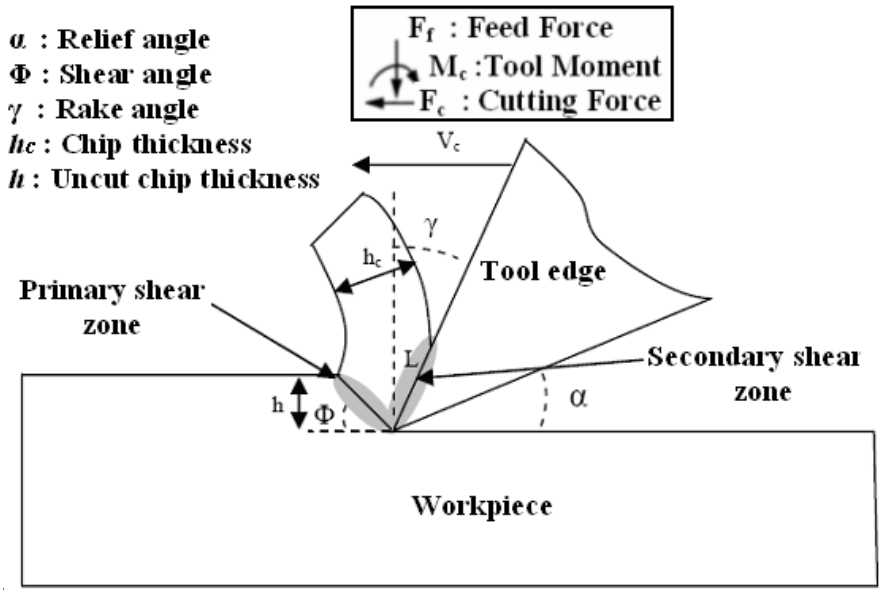

Figure 1. Deformation zones in orthogonal cutting process.

modes, failure criteria, hardening and softening exponent. Finite element analysis (FEA) has been utilized to obtain the insight of chip formation mechanisms since transient stresses and strains can be obtained. However, most of these works on machining are based on 2-D simulation models. In actual machining, such as milling, drilling, turning, boring, face milling and so on, the chip is formed under a 3-D deformation field (obligue machining). FEA is found to be useful to investigate the machining process and chip formation. The literature on metal cutting analysis by the FEM is extensive, and ranges over machining processes, computational approach and models, effects of physical and process parameters, residual stresses, dynamic, chip formation, cutting forces, shear stresses, von mises stresses, chatter(self vibration), predict of tool wear and optimization.

Mackerle (1999, 2003) contains a detailed literature review for machining simulation using the FEM.The employment of which algorithm of simulation and modeling approach is very much dependent upon the type of finite element software that is used. Until the 1995s, over 70% of investigators used finite element code that was written "in-house code" (Ng Eg, 2001), however, the use of public software packages has increased dramatically over the last 10 years. Products on offer that are capable of modeling the metal cutting operation contain ThirdWave AdvantEdge (explicit code) (Özel, 2001, 2003; Kalhori, 2001; Marusich, 2001), DEFORM 3D™ (Ceretti et al., 1996, 1999; Özel and Altan, 2000a,b; Klocke et al., 2001), NIKE2D™(Strenkowski and Carroll, 1985; Carroll and Strenkowski, 1988), ABAQUS/Standard™(Baker et al., 2002; Lei et al., 1999; Shi et al., 2002; Shet and Deng, 2000; Arola and Ramulu, 1997), MARC™(Mamalis et al., 2002; Behrens and Westhoff, 1998), AutoForge (Behrens et al., 2001), FORGE 2D™(Sekhon and Chenot, 1992), ABAQUS™/Explicit(Adibi-Sedeh and Madhavan, 2003; Liu and Guo, 2000; Yang and Liu, 2002; Guo and Liu, 2002; Ng and Aspinwall, 2002; Chuzhoy et al., 2002, 2003), LS DYNA™ [Eulerian-Langrangian-Explicit/Implicit)(Shuyu, 2001; Zhang, 1999) and DYNA3D Explicit (McClain et al., 2002; Wince, 2002), SIMPLE (Langrangian-Implicit-In house code) (Kalhori, 2001), ANSYS/LS DYNA (Langrangian-Explicit) (Lovell et al., 1998; Bağcı et al., 2003). In many of these studies, the numerical codes developed were practical and available commercially for end users.

As metal cutting is mainly a chip formation process, one of the most important considerations when modeling is the approach by which elements of the workpiece material separate as the cuttter advances. In a numerical model of continuum, the material is discretised into finite sections over which, the conversation laws and constitutive equations are solved. The way in which this spatial discretisation is performed leads to different numerical approaches. The approaches used are: Langrangian, Eulerian and ALE (Arbitrary Langrangian-Eulerian).

In the Langrangian approach, the numerical mesh moves and distorts with the physical material as shown in Figure 2.

For Lagrangian based models, these have contained node separation, element deletion and adaptive re-meshing. The main advantages of this approach are that the cutting tool can be simulated from some initial state to steady state cutting and the chip formation together with work-piece residual stress (tensile and compressive) can be forecasted. However, element distortion has been always matter of concern which limited the analysis to incipient chip formation in some studies (Klamecki, 1973;

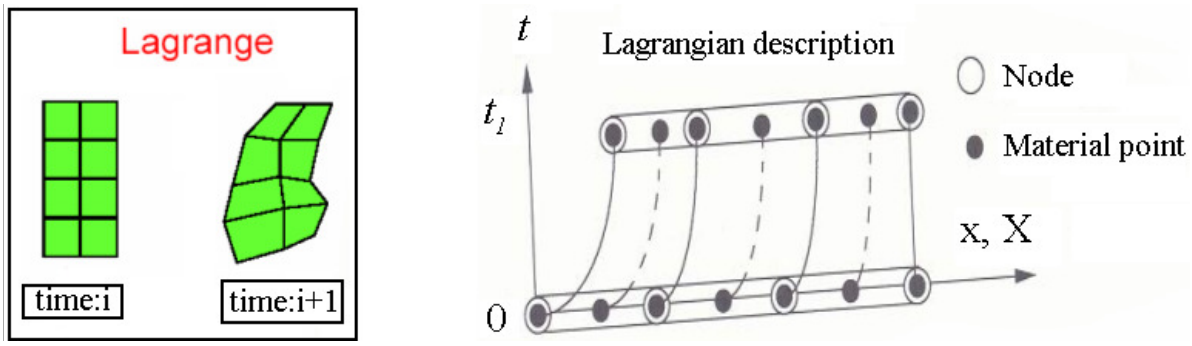

Figure 2. Lagrangian approach.

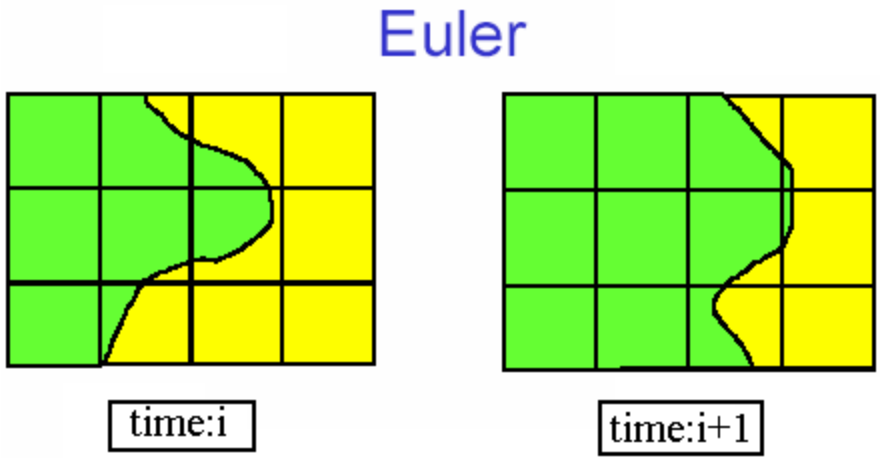

Figure 3. Eulerian approach.

Ceretti et al., 1996, 1999; Özel and Altan, 2000a,b; Klocke et al., 2001; Strenkowski and Carroll, 1985; Sekhon and Chenot, 1992;Usui and Shirakashi, 1982; Komvopoulos and Erpenbeck, 1991;Ueda and Manabe, 1993;Zhang and Bagchi, 1994; Shih et al., 1990; Shih, 1995; Lin and Lin, 1992; Sasahara et al., 1994a, b; Marusich and Ortiz, 1995).

In the Eulerian approach, the numerical mesh is fixed in space and the physical material flows through the mesh as shown in Figure 3.

An Eulerian finite element approach is attractive method for simulating the machining because its mesh is fixed in space, eliminating element distortion problems, and it can create new free surfaces without a special algorithm. However, Eulerian problems require the knowledge of the chip geometry in advance, which, undoubtedly, restricts the range of cutting conditions capable of being analyzed. Some researchers used the Eulerian formulation to model orthogonal metal cutting as continuous chip formation at steady state (Tay and Stevenson, 1974; Carroll and Strenkowski, 1988; Strenkowski and Moon, 1990; Childs and Maekawa, 1990; Childs et al., 1997; Dirikolu et al., 2001;Raczy et al., 2004a,b). Furthermore serrated and discontinuous chip formation can not be simulated. The advantage of using Eulerian formulation is that fewer elements required in modeling the workpiece and the chip, thereby reducing the computation time. The drawback of such an approach was a need in determining chip geometry and shear angle experimentally prior to the simulation.

To take advantage of both descriptions, the ALE description has been put forward, such that the analyst can choose if the mesh should follow material(i.e langrangian) or be fixed (that is, Eulerian). This approach involves a complicated rezoning technique, the rezoning procedure often requires interventions from experinced users as shown in Figure 4.

A mixed Eulerian and Lagrangian formulation has also been proposed (Sekhon and Chenot, 1992) in order to add to the Eulerian formulation the generality of the Lagrangian capability of dealing with transient machining.

In this case, the solution computes nodal velocities under an Eulerian approach which are used to update the nodal coordinates. The Arbitrary Lagrangian Eulerian

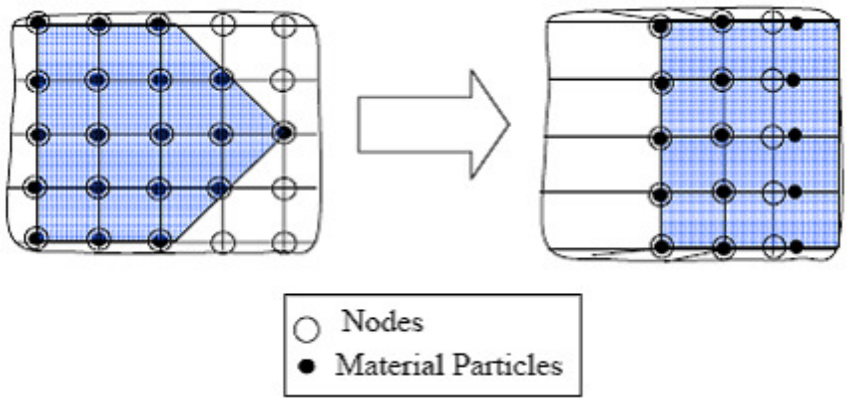

Figure 4. ALE approach.

(ALE) technique combines the best features of the pure Lagrangian analysis (in which the mesh follows the material) and Eulerian analysis (in which the mesh is fixed spatially and the material flows through the mesh). The ALE formulation has been utilized in simulating machining to avoid the frequent remeshing for chip separation (Adibi-Sedeh and Madhavan, 2003; Rakotomalala et al., 1993; Pantale et al., 1996; Olovsson et al., 1999; Movahhedy et al., 2000, 2002; Arrazola et al., 2005). Additionally, the preference of implicit or explicit time integration approaches to solve the equilibrium equations of motion in an FEM analysis is another important consideration for the engineers.

In this paper, a SPH model is presented using a commercially available FEM software package LS-DYNA to simulate the 3-D orthogonal hard part machining process. The aim of this study is to clarify the machining mechanism from the viewpoint of three-dimensional deformation using SPH methodology.

SPH METHODOLOGY

Simulation of machining processes in which the workpiece material is highly deformed (Plastic deformation zone- chip formation process) on metal cutting is a major challenge of FEM codes. The principal problem in using a conventional FE model with langrangian mesh are mesh distortion in the high deformation. Traditional Langrangian approaches such as FEM cannot resolve the large deformations very well. Due to these and other shortcomings of the FEM, so-called meshless, or meshfree methods have recently emerged. These methods rely on constructing interpolation functions at arbitrary discrete points in the domain by enforcing certain reproducing conditions, thereby eliminating the need for elements and a mesh. SPH is a modern effective technique of computer simulation in continuous media mechanics.

SPH is total langrangian and is a truly mesh-free technique initially developed by Gingold and Monaghan (1977) and others for the analysis an simulation of astrophysics problems (Gingold and Monaghan, 1977; Monaghan, 1992). The technique was later extended to model of discontinuous flows with large deformations (Gingold and Monaghan, 1982) and to analysis and simulate for large strain solid mechanics problems (Libersky et al., 1993). Libersky et al. (1993) extended SPH to work with the full stress tensor in 2D. This addition allowed SPH to be used in problems where material strength is important. The development SPH with strength of materials continued with extension to 3D (Libersky et al.,1993), and the linking of SPH with existing finite element codes (Attaway et al., 1994; Johnson, 1994). Review papers by Vignjevic (2004) and Monaghan (1992) cover the early development of SPH. SPH combines the advantages of mesh-free, particle methods and Langrangian. The advantage of the mesh-free method is its capability to solve problems that cannot be influencely solved using other numerical approaches(Idelsohn and Onate, 2006).

The main differences between FEM and SPH are the absence of a grid and in the discretisation of continuum. It does not suffer from the mesh distortion problems that limit Lagrangian methods based on structured mesh when simulating large deformations. Mesh-free is a relatively new numerical technique for the approximate integration of partial differential equations. No direct connectivity exist among particles: the particles are the basis of an interpolator scheme based on the kernel function that is the core of the method and eventually depends on another very important feature of the method: the smoothing length. The value of the smoothing length has to be chosen carefully. Mesh-free technique has several advantages for modelling some industrial mass and heat flows (Li and Liu, 2002).

i. Complex free surface and material interface behaviour, including fragmentation, can be modelled easily and naturally:
ii. The Langrangian framework means that there is no non-linear term in the momentum equation, so the method handless momentum dominated flows very well;
iii. Complicated physics such as multiple phases, realistic equation of state, compressibility, solidification, fracturing, porous media flow, electromagnetics and history dependence of material properties are easy implement (Li and Liu, 2002).

Figure 5 illustrates graphically the similarity between the FE and the SPH approximations. A patch of 9 elements is shown in both the FE and the equivalent SPH approximation. The interpolation functions have been overlaid upon the central element of the FE mesh while the Kernel of the central particle has been "sketched" as spanning its neighbors in the SPH mesh.

Equations

The moving particles are described by;

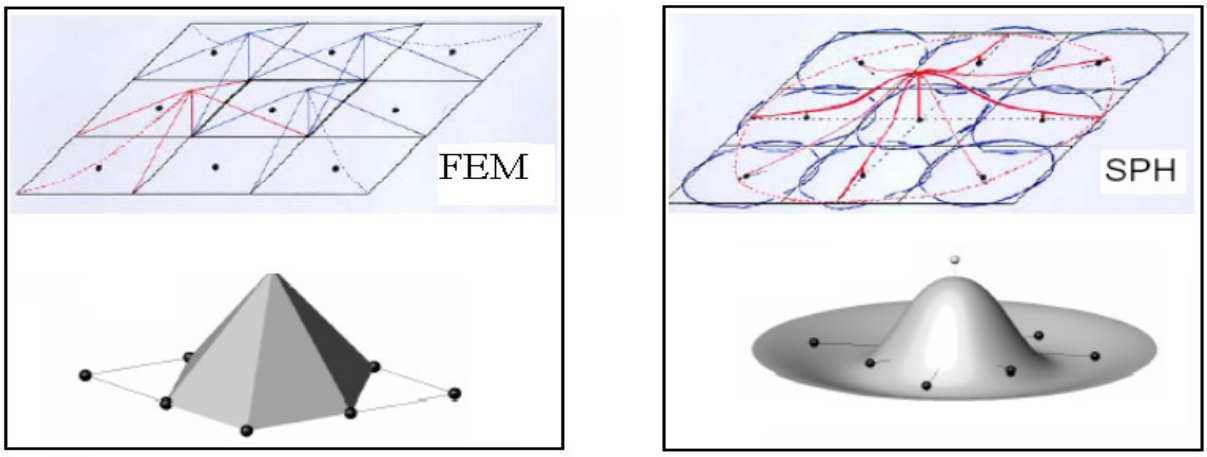

Figure 5. Comparison between FE and SPH modeling of the same patch of 9 elements (Kamoulakos et al., 1997).

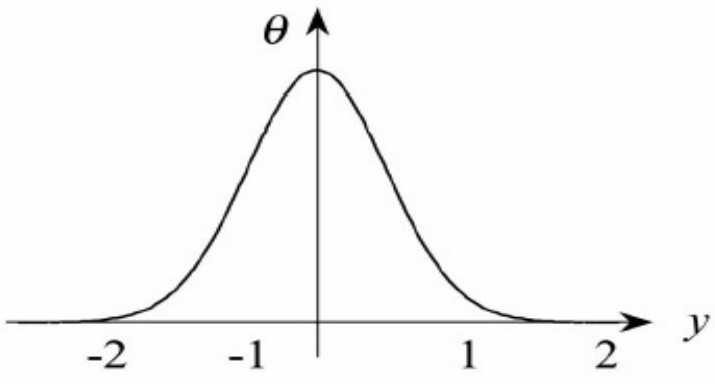

Figure 6. B-Spline function.

$$(\chi_i(t), m_i(t))_{i\in P} \quad [1]$$

Where P is the set of moving particles, xi(t) the location of particle i, and mi(t) the weight of the particle. Lacome (2001a,b), Lacome et al. (2002) and Ls Dyna theoretical manual (Hallquist JO, 1998) presented the movement of each particle and the change of the weight, given by;

$$\frac{dm_i}{dt} = \nabla.V(x_i,t)m_i \quad [2]$$

The quadrature formula can be written as:

$$\int_\Omega f(x)dx \approx \sum_{j\in P} m_j(t) f(x_j(t)) \quad [3]$$

A useful concept in SPH is the smoothing kernel. It is necessary first to introduce the auxiliary cubic B-spline function which has some good properties of regularity.

$$\theta(y) = \alpha_1 x \begin{cases} 1-\frac{3}{2}y^2+\frac{3}{4}y^3 & \text{for } y \le 1 \\ \frac{1}{4}(2-y)^3 & \text{for } 1 \le y \le 2 \\ 0 & \text{for } y \ge 2 \end{cases} \quad [4]$$

Where, α_1 is a constant that depends on dimension and the shape of the kernel function. In two dimensions (Figure 6):

$$\alpha_1 = \frac{10}{7\pi} \quad [5]$$

Lacome (2001a) also suggested the smoothing kernel as:

$$W\left(x_i - x_j, \bar{h}\right) = \frac{1}{h}\theta\left(\frac{x_i - x_j}{\bar{h}}\right) \quad [6]$$

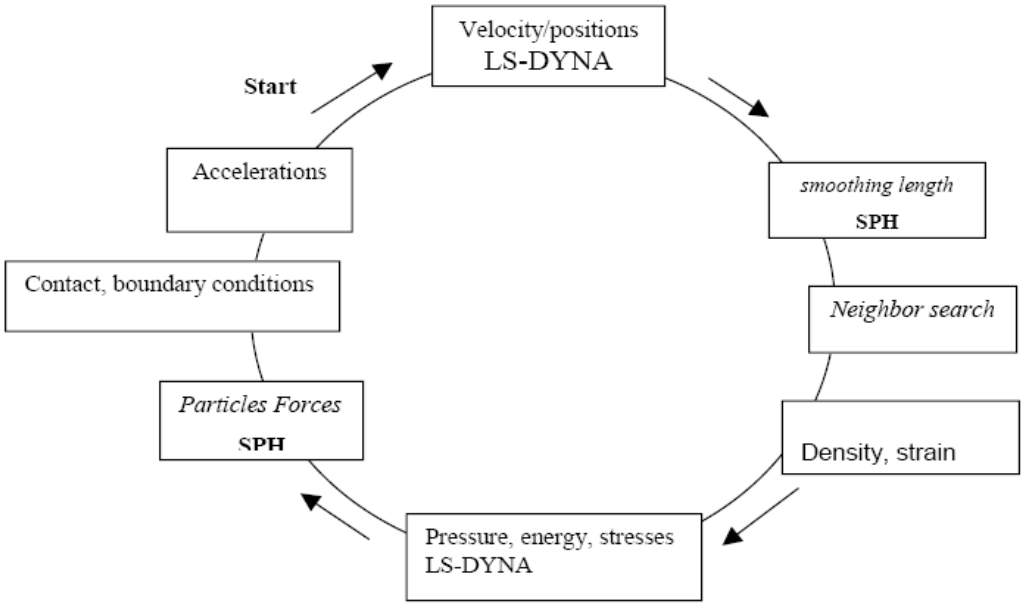

Figure 7. Computational cycle for SPH methodology in LS-DYNA(Lacome et al., 2002).

Where *h* is the smoothing length of the kernel. Generally, a property *A*(*xi*) is represented by its smooth particle approximation $A^h(xi)$ of the function, and by approximating the integral in Equation (7):

$$A^h(x_i) = \sum_{j=1}^{N} m_j \frac{A(x_j)}{\rho(x_j)} W\left(x_i - x_j, \bar{h}\right) \quad [7]$$

The gradient of the function is obtained by applying the operator of derivation on the
smoothing length.

$$\nabla A^h(x_i) = \sum_{j=1}^{N} m_j \frac{A(x_j)}{\rho(x_j)} \nabla W\left(x_i - x_j, \bar{h}\right) \quad [8]$$

Initially in the SPH method, the smoothing length was chosen as constant during the entire simulation. However, it was shown that it is better for each particle to have its own smoothing length, depending on the local number of particles. The current method used for the smoothing length is the gather formulation. In this method, $\bar{h} = h(x_i)$ is defined and the neighboring particles of a defined particle are the particles inside of a sphere centered in *xi* with a radius of $h(x_i)$.

Other equations

The equations for the SPH formulation presented in this section have been described by Monaghan and Lattanzio (1985). The mass density has been defined as:

$$\rho(x) = \sum_{j=1}^{N} m_j W\left(x_i - x_j, \bar{h}\right) \quad [9]$$

The equation of conservation of the mass in a Lagrangian form is:

$$\frac{d\rho}{dt}(x_i) = -\rho \nabla V \quad [10]$$

The SPH approximation for the conservation of mass can be written in two different ways:

$$\frac{d\rho}{dt}(x_i) = \sum_{j=1}^{N} m_j \left(v(x_j) - v(x_i)\right) \nabla W_{ij} \quad [11]$$

The SPH momentum equation may be written as;

$$\frac{dv}{dt}(x_i) = \sum_{j=1}^{N} m_j \frac{\rho}{\rho_j} \left(v(x_j)\right) \nabla W_{ij} \quad [12]$$

Figure 7 illustrates an integration cycle in time of the SPH computation process(Lacome, 2001a). In the SPH analysis, it is important to know which particle will interact with its neighbors because the interpolation depends on these interactions. Therefore, a neighboring search technique has been developed Lacome et al. (2002). The influence of a particle is established inside of a sphere of radius of 2*h*, where *h* is the smoothing length. In the neighboring search, it is also important to list, for each time step, the particles that are inside that sphere. If we have *N* particles, then it is required (*N*-1) distance comparison. If this comparison is done for each particle, then the total amount of comparisons will be *N* (*N*-1). A scheme of this neighbor search is shown in Figure 8 (Lacome et al., 2002).

Smoothing length

The smoothing length *h* is very important in SPH, which has direct

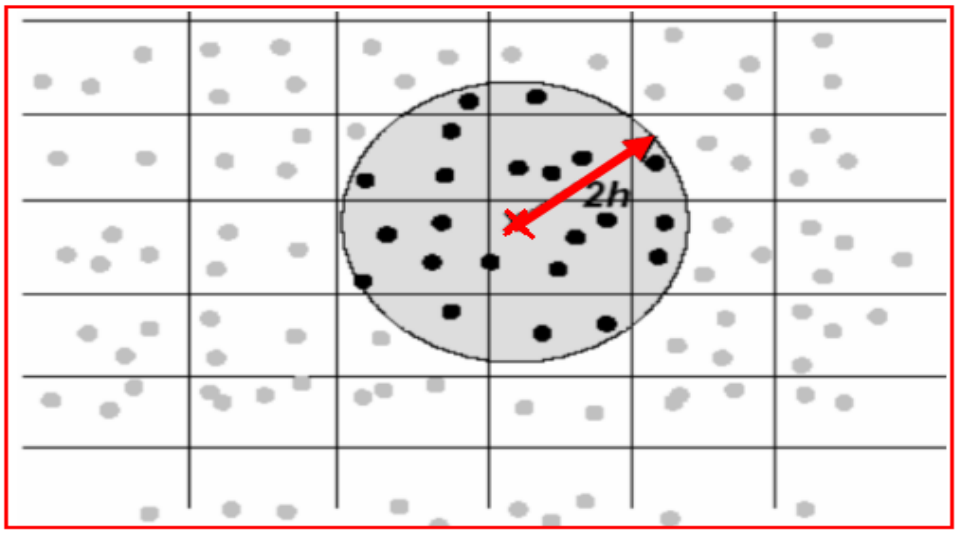

Figure 8. Finding neighbor particles.

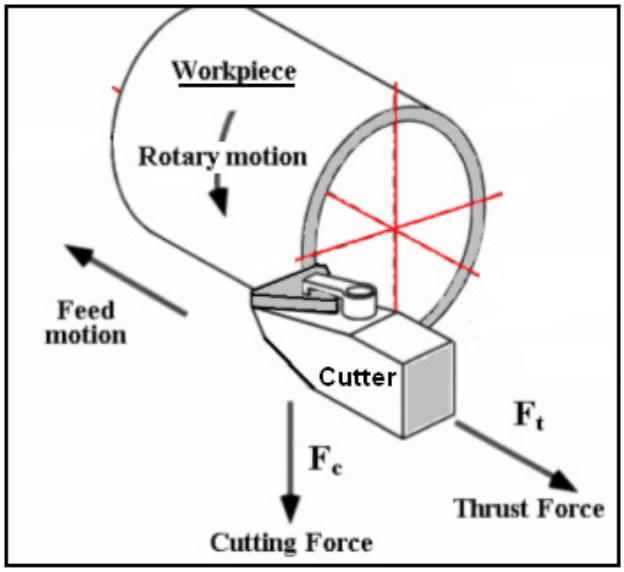

Figure 9. Drawing of orthogonal cutting set-up.

effect on efficiency and accuracy. If *h* is taken too small, there may be not enough particles in the designated range of λ*h* to exert forces on the particle, which results in low accuracy. If the smoothing length is too large, all details of the particle or local properties may be smoothed out, and the accuracy is low, too. The idea is to keep enough particles in the neighborhood to validate the particle approximations of continuum variables. The option of a variable smoothing length is the default in LS-DYNA (Lacome, 2001b). The time rate of change for smoothing length is given by the following equation:

$$\frac{dh}{dt} = \frac{1}{3}\bar{h}\nabla.V \qquad [13]$$

Table 1. Cutting conditions and tool geometry.

Feed (mm/rev)	0.05
Rake angle (°)	-5
Clearance angle (°)	5
Cutting Speed (m/min)	200, 300

MODELLING OF 3-D ORTHOGONAL CUTTING

FEM simulations were conducted in this study with the same experimental conditions employed by literature (Ozel, 2003). Figure 9 shows the orthogonal experimental set-up. The tool geometry and the cutting conditions used for this simulation are listed in Table 1. The workpiece material was AISI H13 die steel (52 HRc), tool was CBN insert. Other material physical properties for the tools and workpiece are listed in Table 2.

Process parameters

The tool geometry and the cutting conditions used for the orthogonal metal cutting simulation are presented in Table 1 and Figure 10.

Initial setup and steps of SPH method for cutting simulation

In a SPH calculation, one needs to initially specify particle masses, positions, velocities and other physical quantities. All of these except positions and masses are usually straigth forward to specify. Firstly, we use three-dimensional solid CAD models to describe the workpiece and cutter geometry using CATIA R17. Secondly, CAD models were export to ANSYS finite element software for definition of contacts, material properties, etc. Thirdly, LS-DYNA input file was

Table 2. The mechanical and physical properties of the AISI H13 workpiece material.

Youngs modulus (MPa)	211,000
Poissons ratio	0.28
Density (kg/m^3)	7800
Thermal conductivity (W/m K)	37
Specific heat (J/kg K)	560
Hardness (HV)	544
Heat transfer coefficient (N/s/mm/C)	40
Shear flow stres, k(MN m^{-2})	1033
Q/R	0.113
Strain hardening sensitivity (n)	0.15
Composition	C, 0.94% Si, 0.33% Mn, 5.02% Cr, 1.35% Mo, 0.98% V, 0.12% Ni, Fe

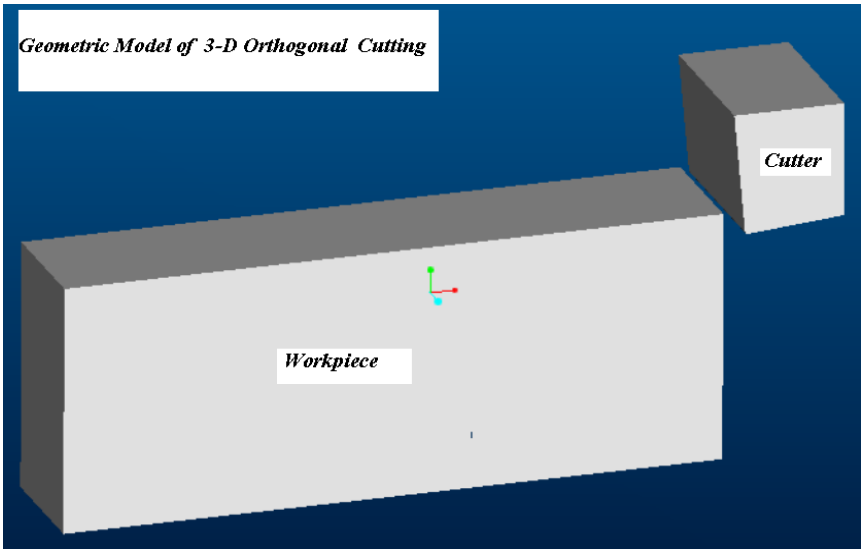

Figure 10. Geometric model of 3-D orthogonal cutting.

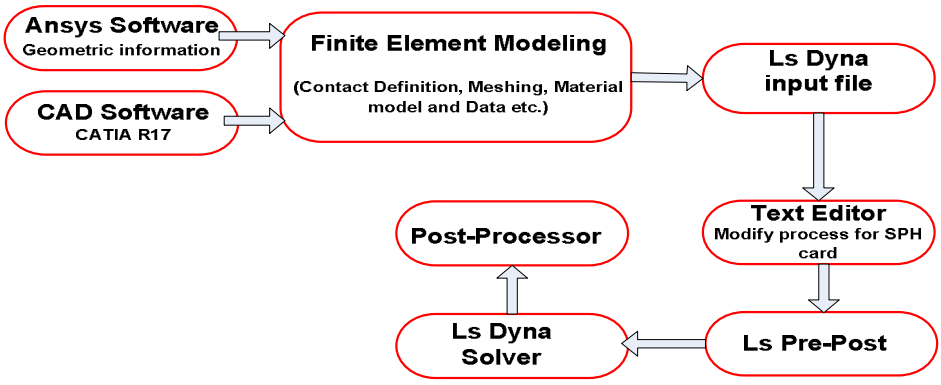

Figure 11. Modelling steps for cutting simulation in Ls-Dyna.

generated with ANSYS software and modified using text editor as shown in Figure 11.

This surface mesh is converted into the initial set-up for SPH particles using an in commercial pre-processor. In this step, the

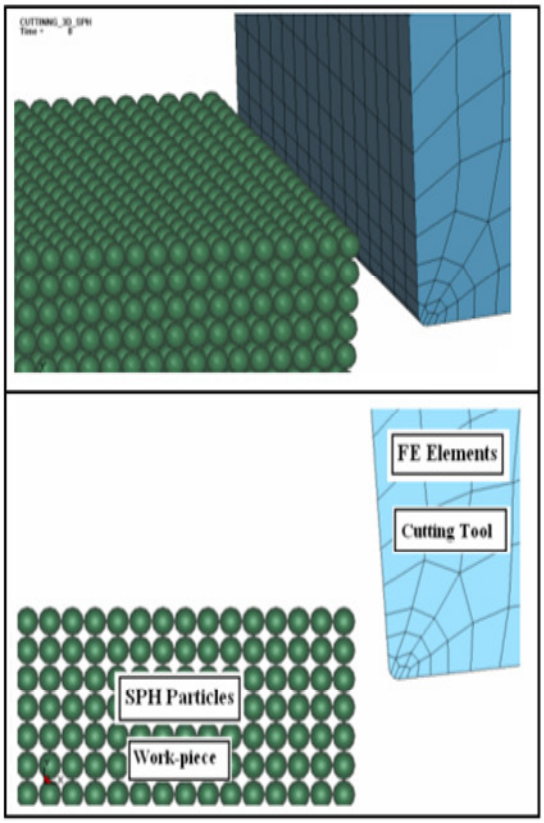

(a)

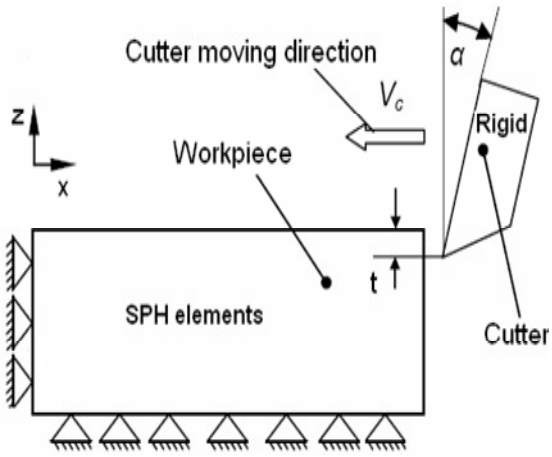

(b)

Figure 12. (a) Initial FEM model of workpiece and tool; **(b)** The model with constraints.

nodes of the surface mesh become the positions of the SPH boundary particles. Boundary normals are calculated and assigned to the resulting boundary particles. Particles in the SPH method carry information about their hydrodynamic and thermodynamic information, this in addition to the mass needed to specify the evolution of the fluid. Nodes in SPH are similar to nodes in a mesh, the difference is that these nodes are continuously deformable and distort automatically to put more of the computational effort in regions of relatively high density. The only requirement for the mesh is that the node spacing be fairly close to uniform. The actual mesh type is unimportant, since the mesh will be discarded as part of the conversion to SPH particles.

Some initials characteristics and properties for the SPH simulations have to be defined for the user. There is no need to define contact between SPH parts. This contact will only be defined between two SPH materials when one particle of one material is inside the sphere of influence of the other SPH material (Hallquist JO, 1998). For all particles, masses are calculated, material properties and other state variables are set to give the complete initial setup for SPH simulation. The workpiece was modeled with SPH particles since it undergoes large deformations during the machining. The tool was supposed to be not deformable and its velocity was imposed. The analysis was performed with a constant speed of the tool in the x direction, as shown in Figure 12. The tool has the same geometry as the tool used in the experiments. A comparison between the numerical analysis and the experiments is described in the result and discussion.

Material constitutive model for workpiece

Plastic kinematic hardening model is a strain-rate dependent elastic-plastic model. Plastic kinematic model constants for AISI H13 steel are given in Table 2. Isotropic, kinematic, or a combination of isotropic and kinematic hardening models with strain rate dependency and failure. Isotropic and kinematic contributions may be varied by adjusting the hardening parameter β between 0 (kinematic hardening only) and 1 (isotropic hardening only). Strain rate is accounted for using the Cowper-Symonds model which scales the yield stress by the strain rate dependent factor as shown below (Figure 13):

$$\sigma_Y = \left[1 + \left(\frac{\dot{\varepsilon}}{C}\right)^{\frac{1}{P}}\right](\sigma_0 + \beta E_p \varepsilon_p^{eff}) \quad [14]$$

Where σ_0 is the initial yield stress, $\dot{\varepsilon}$ is the strain rate, C and P are the Cowper-Symonds strain rate parameters, $\varepsilon_p$eff is the effective plastic strain, and E_p is the plastic hardening modulus which is given by:

$$E_p = \frac{E_{tan} E}{E - E_{tan}}. \quad [15]$$

RESULTS AND DISCUSSION

The cutting model and cutting conditions mentioned above for orthogonal cutting process have been performed. The cutting tool contacts with an initially uncut workpiece and moves forward incrementally until a steady state of chip formation is being achieved, so that the cutting process can be investigated in detail.

Analysis of equivalent plastic strain rate

The cutting tool is advanced incrementally into the work-piece and the chip is formed gradually until the

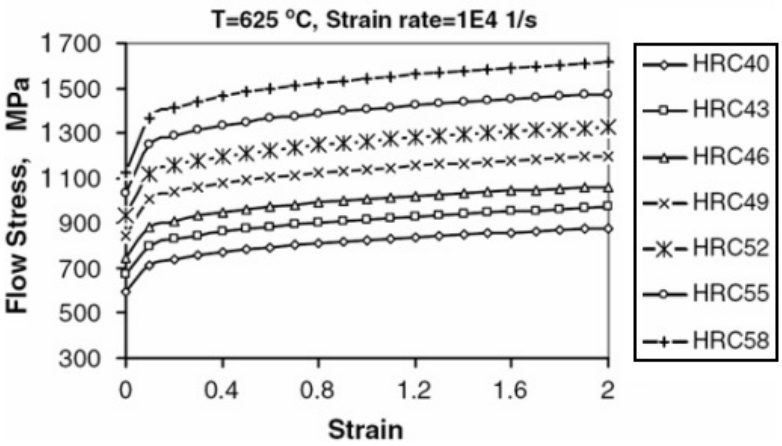

Figure 13. Flow stress data for AISI H13 die steel at its different hardness (Yan et al., 2007).

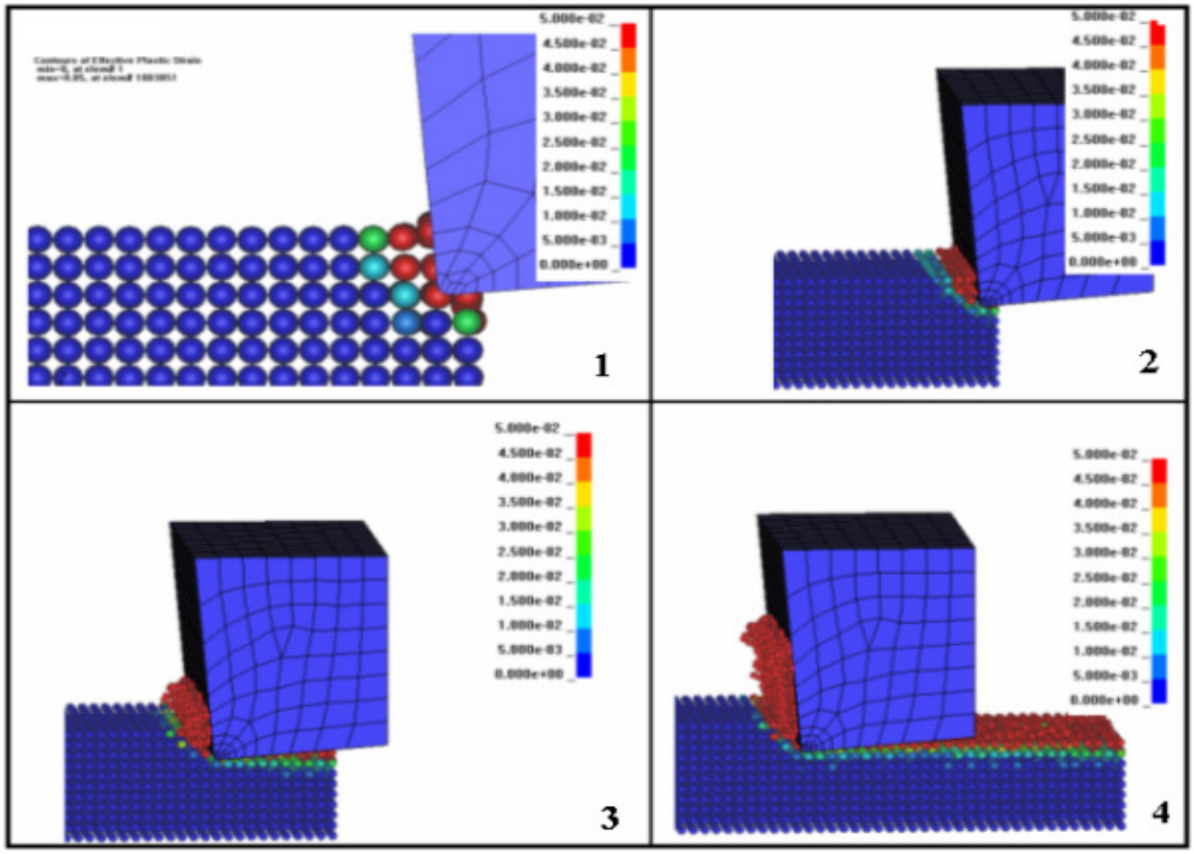

Figure 14. Equivalent plastic strain rate for different time steps.

steady-state is attained, that is, the cutting force reaches a constant value. The cutting force, as well as the effective stress, the maximum shear stress and the equivalent plastic strain are obtained for orthogonal cutting simulation case mentioned. As shown in Figure 14. High strain-rates are obtained along the primary deformation zone, with a maximum value obtained at the tool tip region.

Analysis of equivalent plastic strain

The distribution of the equivalent plastic strain in the chip and workpiece are shown in Figure 15. The strain is

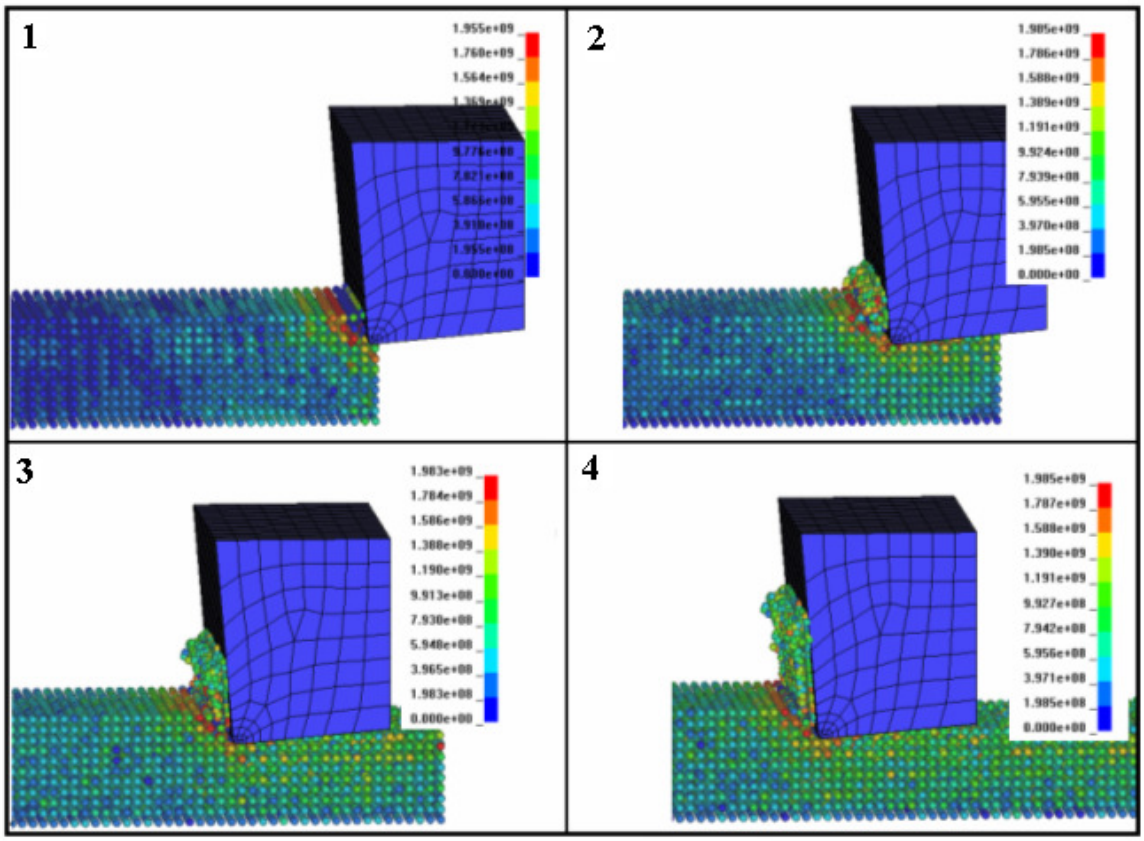

Figure 15. The distribution of equivalent strain in the workpiece and the chip for different steps.

concentrated between the tool tip and the rake face. The higher equivalent stress appears in the primary deformation zone, and a large plastic deformation also exists around this zone.

Analysis of effective stress

Contours of effective stress during machining simulation are shown in Figure 16. An indicative effective stress distribution, as obtained from simulation case 1, is shown in Figure 16. The highest effective stress was observed along the primary shear zone, partly extended, along the secondary shear zone, near the tool tip, where sticking friction conditions prevail. The cutter enters into cut, the cutting edge is subjected to a shock load, which depending upon the chip cross-section, workpiece material, cutting speed and type of cut and etc.

Analysis of shear stress

A typical shear stress distribution for case 1 is shown in Figures 17 and 18. The highest shear stresses predicted are of a compressive nature and appeared along the primary deformation zone, that is the shear zone, whilst the maximum shear-stress observed at the tool edge radius, indicating that, material separation takes place at this area.

Comparison between experiments and analyses for cutting forces

In this study, the cutting forces are predicted by the FEM-based code Ls-Dyna using the SPH methodology. The predicted results from the present study are compared with experimental observations and Lagrangian finite element analysis results available in the literature (Ozel, 2003). He is studied and compared to experimental results and numerical FEM (AdvantEdge) results. AdvantEdge is a reference in machining simulations. It is an explicit dynamic, thermo-mechanically coupled FEM package specialized for metal cutting. It can be observed that the forces predicted in the present study are in reasonable agreement with the published experimental results. In this paper the concentrated was on the cutting force, because it is the force which typically is the most important regarding fixation in the lathes and the CNC milling machines.

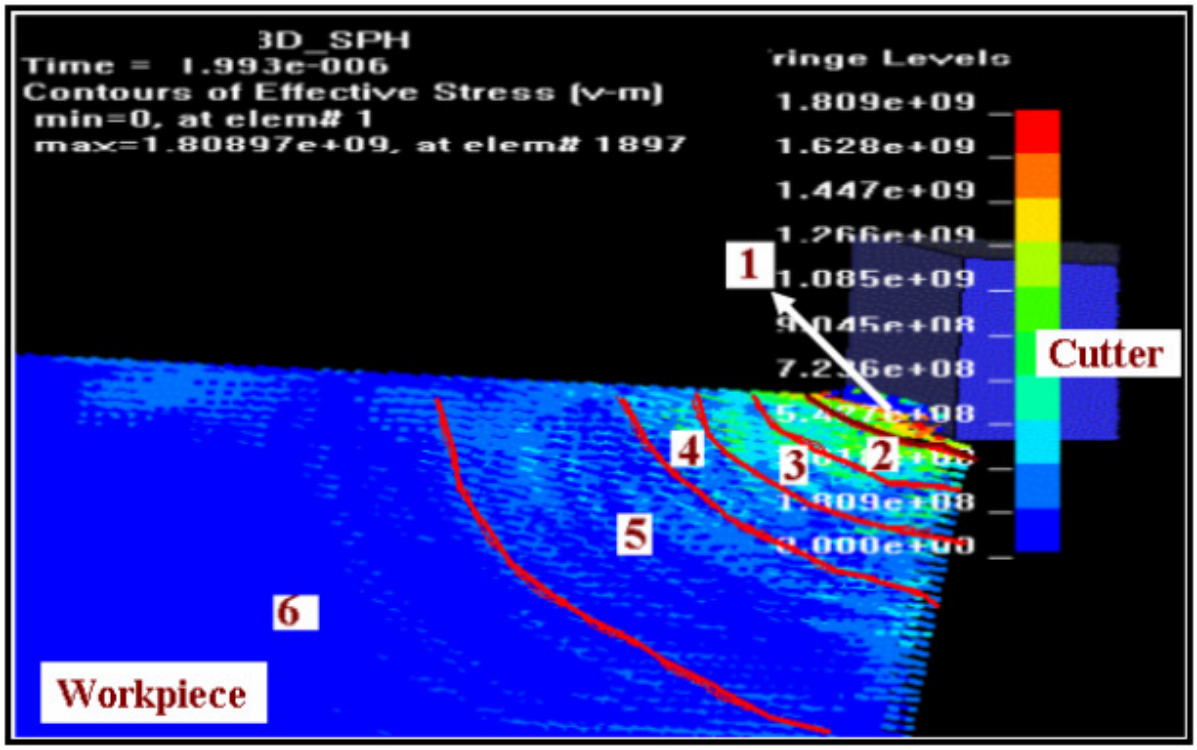

Figure 16. The contours of effective stress in the workpiece.

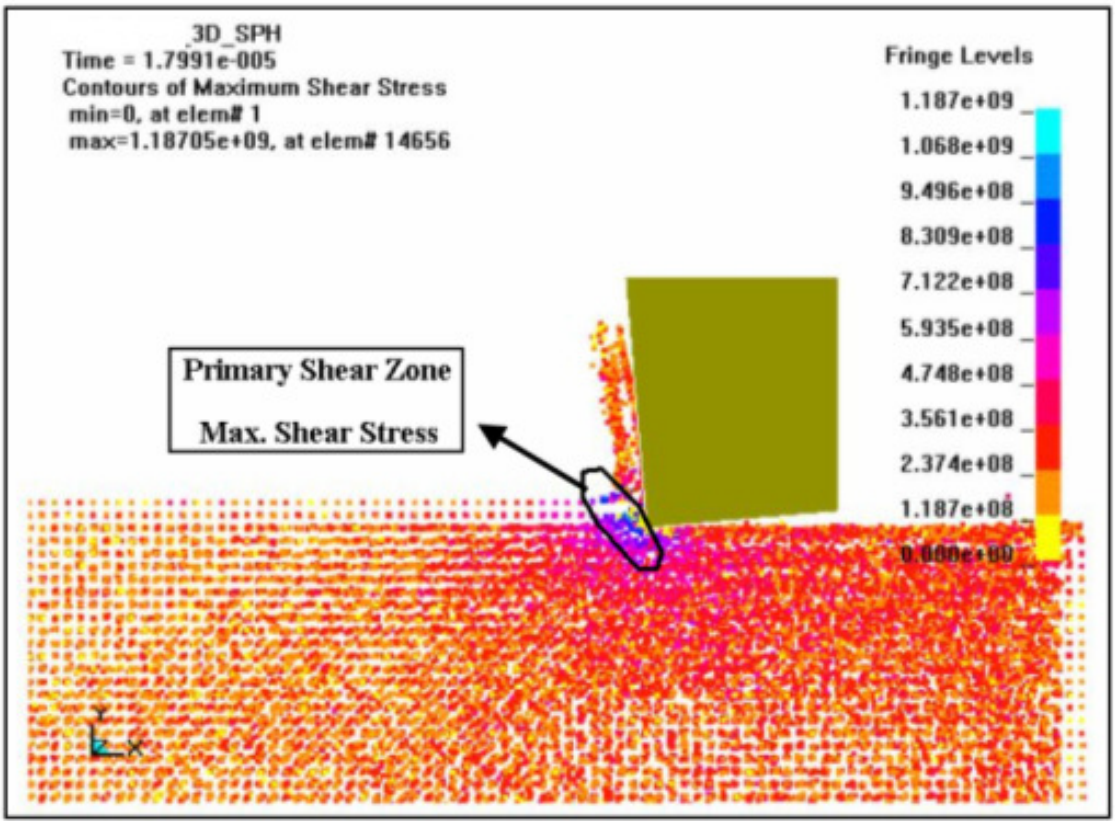

Figure 17. The contours of max. shear stress in the workpiece.

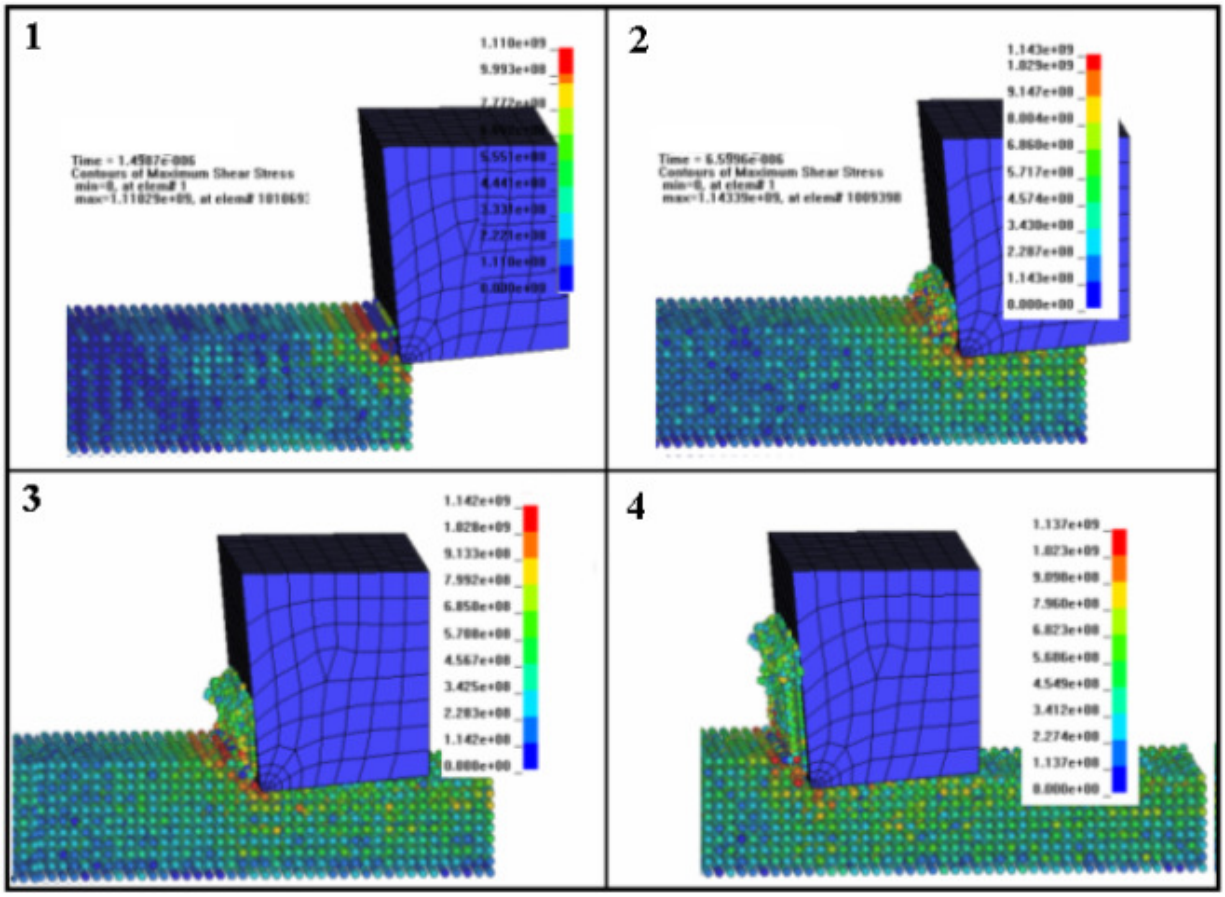

Figure 18. The contours of maximum shear stress in the workpiece for different time steps.

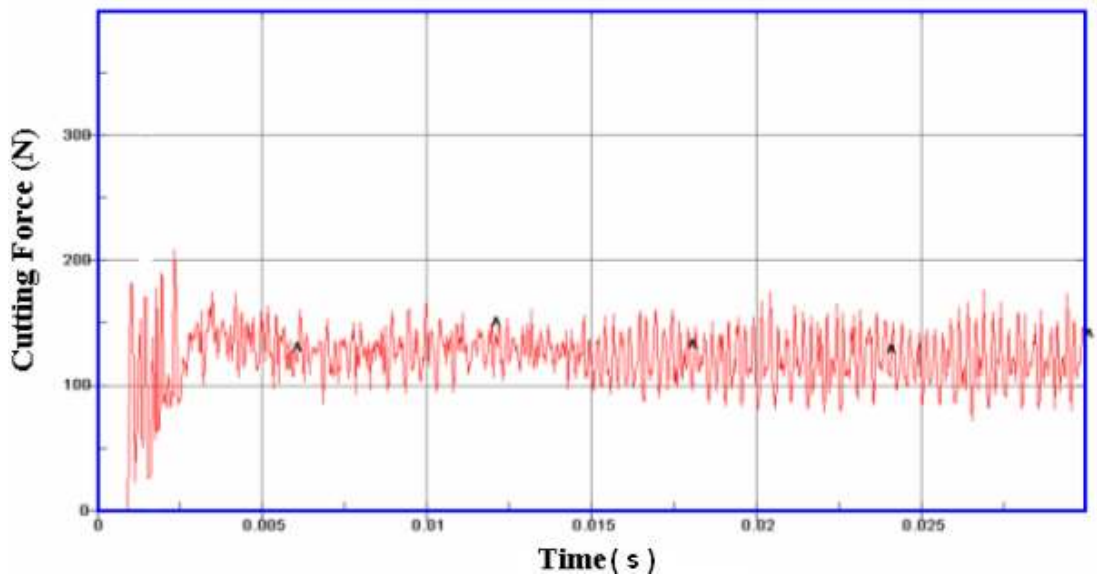

Figure 19. Cutting force graph for V_c = 200 m/min and f = 0.05 mm/rev conditions.

The variation of the simulated cutting forces with tool travel for f = 0.05 mm/rev and V_c=200 mm/min is shown in Figure 19. There is a short period increase of the main cutting force component during entrance of the tool

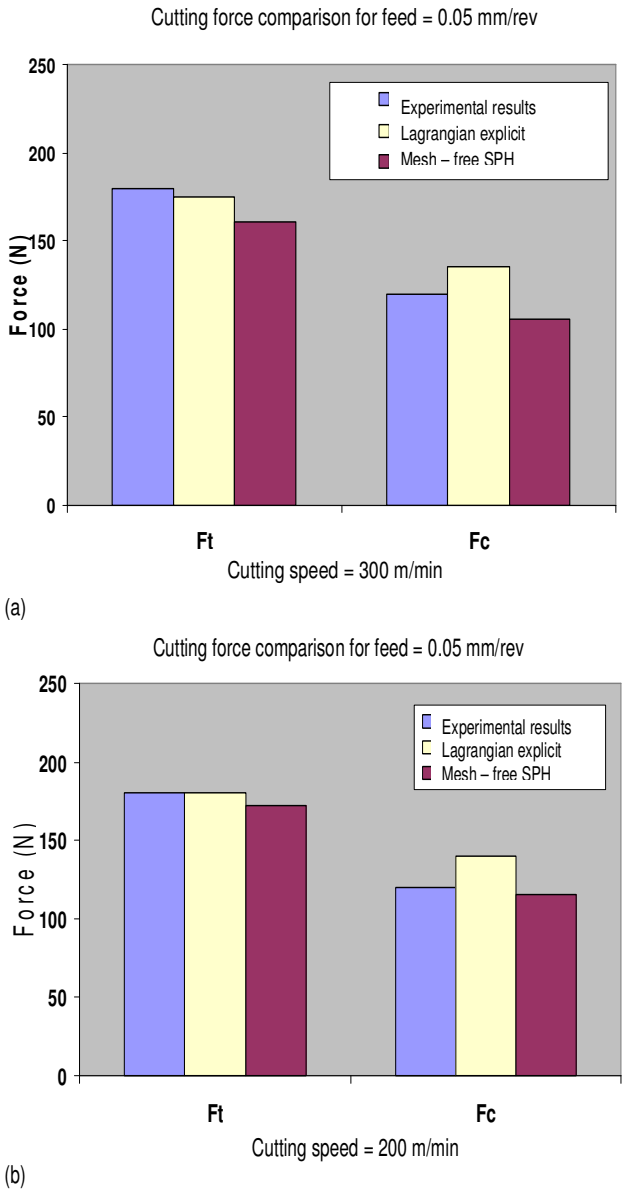

Figure 20. Comparison of cutting forces of predicted SPH and published results.

cutting edge into a work piece. This increase can exceed a mean value several times after entrance of the cutting tool (cut in). Some seconds was taken to keep high temperature during hard turning cut-in process and then the cutting forces would be decrease due to the metal soften effect as shown Figure 19.

The experimental cutting force at steady state under the same cutting conditions, taken from literature, is also shown in Figure 20. The predicted of mesh-free SPH cutting forces agree within 8.43% and 11.70% of the measured values for tangential and normal components respectively, which may be observed as an acceptable level of agreement. Villumsen and Fauerholdt (2008) and Limido et al. (2007) perform ananalysis with the meshless SPH method in the FEM code LS-DYNA. In Limido et al. (2003) paper, cutting forces from experiments are compared with cutting forces form numerical analysis. The variation between the estimated and experimentally measured forces is 10% for the cutting force and 30% for the thrust force. Villumsen and Fauerholdt (2008) achive to predict the cutting forces with a 8.4% deviation of cutting force and a 12% deviation of the thrust force compared to the measured forces. These differences can be interpreted by chip separations criteria, selection of material model, friction modelling approach and SPH velocity assumption. The work-piece will be modeled using "Johnson Cook" material model as that of 3D cutting simulations which the material model will show the dependency of flow stress on strain rates and temperatures which are near to the realistic conditions rather than plastic kinematic hardening material model. By adjusting and adapting the parameters of friction coefficient by a systematic study it is probably to align the variations, at a higher value of the friction coefficient the force values will be raise. The orthogonal cutting forces values will then be less under-estimated.

Conclusions

The application of SPH method is fairly new in metal cutting simulations. Its features are not fully understood and the most effective means to exploit it are still being discovered. Despite its newness, the SPH method can be seen to be a very promising tool for the study of machining. SPH method has been shown hereto overcome the major difficulties of cutting simulation that obstruct finite element simulation of these processes. Most importantly, this method is a tool that permits the study of the large deformations that occur near the cutting tool without the loss of accuracy and stability associated with finite element analysis of these problems.

In this paper, the orthogonal cutting process of AISI H13 steel material were modeled and analysed using SPH method. Equivalent plastic strain rate, equivalent plastic strain, effective stress, shear stress and cutting forces were simulated and obtained for orthogonal cutting simulation cases above mentioned. The developed SPH model gained its ability to correctly estimate the cutting forces, as illustrated in two orthogonal cutting cases. Ls Dyna predicted cutting forces values agree within 8.43% and 11.70% of the experimental measured values for tangential and normal components respectively, which may be considered as an acceptable level of agreement. These variations can be clarified by chip separations criteria, material modelling, friction model and SPH velocity assumption. Additionally, next paper will be focused on examination and prediction of realistic chip generation and frictional behaviour in cutting process using the SPH method.

REFERENCES

Adibi-Sedeh AH, Madhavan V (2003). Understanding of finite element analysis results under the framework of Oxley's machining model. 6th CIRP Int. Workshop on Modeling of Machine Operation. Canada.

Arola D, Ramulu M (1997). Orthogonal Cutting of Fiber-Reinforced Composites:A Finite Element Analysis. J. Mech. Sci.,. 39: 597-613.

Arrazola PJ, Ugarte D, Montoya J, Villar A, Marya S (2005). Finite element modeling of chip formation process with Abaqus/Explicit 6.3. COMPLAS - 2005.

Attaway SW, Heinstein MW, Swegle JW (1994). Coupling of smooth particle hydrodynamics with the finite element method. Nucl. Eng. Design, 150: 199-205.

Bağcı E, Özçelik B, Kurtaran H(2003). Metal Kesmenin Sonlu Elemanlar Yöntemi ile Analizinde Kullanılan Yazılımlar, Modellemede Karşılaşılan Güçlükler ve Algoritmaların Yetersizlikleri. Makina Tasarım ve İmalat Teknolojileri Kongresi. Konya-TURKEY.

Bäker M, Rösler J, Siemers C (2002). A Finite Model of High Speed Metal Cutting with Adiabatic Shearing. Comp. Struct., 80: 495-513

Behrens A, Westhoff B (1998). Anwendug von Marc auf Zerspanprozesse. Laboratorium Fertigungstechnik. MARC Benutzertreffen- München.

Behrens A, Westhoff B, Kalisch K (2001). Investigation of Segmented Chip Forming in High Speed Cutting Processes. Inst. of Des. Prod. Eng. Univ. Federal Armed Forces. Germany,

Carroll JS, Strenkowski JT (1988). Finite Element Models of Orthogonal Cutting with Application to Single Point Diamond Turning. J. Mech. Sci., 30: 899-920

Ceretti E, Fallböhmer P, Wu WT, Altan T (1996). Application of 2D FEM to chip formation in orthogonal cutting. J. Mat. Pro. Technol., 59:169–181.

Ceretti E, Lucchi M, Altan T (1999). FEM simulation orthogonal cutting: serrated chip formation. J. Mater. Pro. Technol., 95: 17–26.

Childs THC, Maekawa K (1990). Computer-aided simulation and experimental studies of chip flow and tool wear in the turning of low alloy steels by cemented carbide tools. Wear, 139: 235–250.

Childs THC, Dirikolu MH, Sammons MDS, Maekawa K, Kitagawa T (1997). Experiments on and Finite Element Modeling of turning free-cutting steels at cutting speeds up to 250 m/min. Proceedings of 1st French and German Conference on High Speed Machining. pp. 325–331.

Chuzhoy L, DeVor RE, Kapoor SG (2003). Machining simulation of ductile iron and its constituents. Part 2: numerical simulation and experimental validation of machining. ASME J. Manu. Sci. Eng., 125:192–201.

Chuzhoy L, DeVor RE, Kapoor SG, Bammann DJ (2002). Microstructure-level modeling of ductile iron machining. ASME J. Manuf. Sc. Eng., 24: 162–169

Dirikolu MH, Childs THC, Maekawa K (2001). Finite element simulation of chip flow in metal machining. Int. J. Mec. Sci. , 43: 2699–2713.

Ersnt H, Merchant ME (1941). Chip formation, friction and high quality machined surfaces. Trans. Am. Soc. Metals (ASM), 29: 299-378.

Gingold RA, Monaghan JJ (1982). Kernel estimates as a basis for general particle methods in hydrodynamics. J. Comp. Phys., 46: 429-453.

Gingold RA, Monaghan JJ(1977). Smooth particle hydrodynamics: theory and application to non-spherical stars. Mon. Not. R. Astron. Soc., 181: 375-389.

Guo YB,Liu CR (2002). 3D FEA modeling of hard turning. J. Man. Sci. Eng., 124: 189–199.

Hallquist JO (1998). LS-DYNA Theoretical Manual. LSTC, Livermore, CA, USA.

Idelsohn SR, Oñate E (2006). To mesh or not to mesh. That is the question… Comp. Methods Appli. Mech. Eng. , 195(37-40): 4681-4696.

Johnson GR (1994). Linking of Lagrangian particle methods to standard finite element methods for high velocity impact computations. Nucl. Eng. Design, 150: 265-274.

Kalhori V (2001). Modelling and Simulation of Mechanical Cutting. PhD Thesis. LTU-Sweden.

Kamoulakos A, Przybylowicz M, Groenenboom P (1997). Smoothed Particle Hydrodynamics for Space debris Impact Simulations - An Approach With the PAM-SHOCK Transient Dynamics Code. Int. Workshop in New Models and Num. Codes for Shock Wave Proces. in Condensed Media. Oxford, UK.

Klamecki BE (1973). Incipient chip formpation in metal cutting-a three dimension finite element analysis. PhD. Dissertation. University of Illinois-Urbana-Champaign.

Klocke F, Raedt HW, Hoppe S (2001). 2D-FEM simulation of the orthogonal high speed cutting process. Mach. Sci. Technol.. 5(3): 323–340.

Komvopoulos K, Erpenbeck SA (1991). Finite element modeling of orthogonal metal cutting. ASME J. Eng. Industry, 113: 253–267.

Lacome JL (2001a). Smoothed Particle Hydronamics Part:I. FEA Newsletters. pp. 3-8.

Lacome JL (2001b). Smooth Particle Hydrodynamics-Part II. FEA Newsletters. pp. 6-11.

Lacome JL (2002). Smoothed particle hydrodynamics (SPH): A New Feature In LS-DYNA. 7th International LS-DYNA Users Conf. Dearborn, Michigan. 7: 29–34.

Lacome JL, Espinosa Ch, Gallet C (2002). Simulation of Hypervelocity Spacecrafts And Orbital Debris Collisions using Smoothed Particle Hydrodynamics in LS-DYNA. 5th Cranfield DCSSS Conf.UK.

Lee EH, Schaffer BW (1951). The theory of plasticity applied to a problem of machining. J. Appl. Mech,. 18(4): 405.

Lei S, Shin YC, Incropera FP(1999). Thermo-mechanical Modeling of Orthogonal Machining Process by Finite Element Analysis. Int. J. Mac. Tools Man, 39: 731-750.

Li S, Liu WK (2002). Meshfree particle methods and their applications. App. Mech. Rev., 54:1-34.

Libersky LD, Petschek AG, Carney TC, Hipp JR, Allahadi FA (1993). High Strain Lagrangian Hydrodynamics: A Three-Dimensional SPH Code for Dynamic Material Response. J. Comp. Phys., 109(1): 67-75.

Limido J, Espinosa C, Salaun M (2007) SPH method applied to high speed cutting modeling. Int. J. Mech. Sci., 49: 898-908.

Lin ZC, Lin SY (1992). A couple finite element model of thermo-elastic-plastic large deformation for orthogonal cutting. ASME J Eng. Ind., 114: 218–226.

Liu CR, Guo YB (2000). Finite element analysis of the effect of sequential cuts and tool-chip friction on residual stresses in a machined layer. Int. J. Mech. Sci., 42: 1069–1086.

Lovell MR, Bhattacharya S, Zeng R (1998). Modeling orthogonal machining process for variable tool-chip interfacial friction using explicit dynamic finite element methods. Proc. of the CIRP Int. Workshop on Modeling of Machining Operations. pp. 265–276.

LS-DYNA (2006). Keyword User's Manual V970. Livermore Soft. Techno. Comp.. ISBN: 0-9778540-2-7.

Mackerle J (1999). Finite element analysis and simulation of machining: a bibliography (1976–1996). J. Mat. Pro. Technol., 86: 17–44.

Mackerle J (2003). Finite element analysis and simulation of machining: an addendum a bibliography (1996–2002). J. Mater. Pro. Technol., 43: 103–114.

Mamalis AG, Branis AS, Manolakos DE (2002). Modelling of Precision Hard Cutting using implicit Finite Element Methods. J. Mater. Proces. Technol., 123:464-475.

Marusich TD, Ortiz M (1995). Modeling and simulation of high-speed machining. Int. J. Num. Methods Eng., 38: 3675–3694.

Marusich TD (2001). Simulation and Analysis of Chip Breakage in Turning Processes. (http://thirdwave.com).

McClain B, Batzer SA, Maldonado GI (2002). A Numeric investigation of the Rake Face Stress Distribution in Orthogonal Machining. J. Mater. Process. Technol.123: 114-119.

Monaghan JJ (1992). Smoothed particle hydrodynamics Ann. Rev. Astron. Astrophys, 30- 543.

Monaghan JJ, Lattanzio JC (1985). A refined particle method for astrophysical problems. Astro. Astrophys., 49: 135-143.

Movahhedy MR, Altintas Y, Gadala MS (2002). Numerical analysis of metal cutting with chamfered and blunt tools. J. Man. Sci. Eng., 124: 178–188.

Movahhedy MR, Gadala MS, Altintas Y (2000). FE Modeling of Chip Formation in Orthogonal Metal Cutting Process: An ALE Approach. Mach. Sci. Technol., 4:15–47.

Ng EG, Aspinwall DK (2002). Modeling of hard part machining. J. Mat. Proc. Technol., 124: 1–8.

Ng EG (2001). Modelling of the cutting process when machining hardened steel with PCBN tooling. PhD Thesis. UK.
Okushima K, Kakino Y (1971). The residual stress produced by metal cutting, Ann. CIRP. 20(1): 13-14.
Olovsson L, Nilsson L, Simonsson K(1999). An Ale formulation for the solution of two-dimensional metal cutting problems. Comp. Structures, 72: 497–507.
Özel T (2001). Investigation of the influence of Edge Preparation on CBN Cutting Tools when Machining Hardened AISI H-13 Tool Steel. 2nd Int.Conf. on Design and Prod. of Dies and Molds.
Özel T (2003). Modelling of Hard Part Machining: Effect of insert Edge Preparation in CBN Cutting Tools. J. Mat. Pro, Technol., 141(2): 284-293
Özel T, Altan T (2000a). Determination of workpiece flow stress and friction at the chip-tool contact for high-speed cutting. Int. J. Mach. Tools Manufac., 40 (1): 133–152.
Özel T, Altan T (2000b). Process simulation using finite element method- prediction of cutting forces, tool stresses and temperatures in high-speed flat end milling process. Int. J. Mach.Tools Manufac., 40(5): 713–738.
Pantale O, Rakotomalala R, Touratier M, Hakem N (1996). A three-dimensional numerical model of orthogonal and oblique metal cutting processes. Proc. of Eng. Sys. Des.and Analy. ASME. 3: 199–206.
Raczy A, Elmadagli M, Altenhof WJ, Alpas AT (2004). An Eulerian Finite-Element Model for Determination of Deformation State of a Copper Subjected to Orthogonal Cutting. Symp. on the Magic of Materials: Structures and Properties. 35A(8): 2393-2400.
Raczy A, Altenhof W, Alpas AT (2004). An Eulerian Finite Element Model of the Metal Cutting Process. 8th Int. LS-DYNA Users' Conf. Dearborn- MI.USA. 9-26.
Rakotomalala R, Joyot P, Touratier M (1993). Arbitrary Lagrangian-Eulerian thermomechanical finite element model of material cutting. Comm. in Numerical Meth.in Eng., 9: 975–987.
Sasahara H, Obikawa T, Shirakashi T (1994a). FEM analysis on three dimensional cutting. Int. J. Japanese Soc. Precision Eng., 28(2): 473–478.
Sasahara H, Obikawa T, Shirakashi T (1994b). The prediction of effects of cutting condition on mechanical characteristics in machined layer. Advancement of Intelligent Prod. JSPE. 473–478.
Sekhon GS, Chenot JL (1992). Some simulation experiments in orthogonal cutting. Num. Methods in Ind. Forming Processes. 901–906.
Shet C, Deng X(2000). Finite Element Analysis of the Orthogonal Metal Cutting Process. J. Mat. Proces. Technol. 105: 95-109.
Shi G, Deng X, Shet C (2002). A Finite Element Study of the Effect of Friction in Orthogonal Metal Cutting. Finite Elements Anal. Design, 38: 863-883.
Shih AJ, Chandrasekar S,Yang HT (1990). Finite element simulation of metal cutting process with strain-rate and temperatures effects. Fundamental Issues in Machining- ASME- PED. 43: 11–24.
Shih AJ (1995). Finite element simulation of orthogonal metal cutting. ASME J. Eng. Ind., 117:84-93.
Shuyu B (2001). A Finite Element Model of Face Milling. CODEF. (http://lma.berkeley.edu).
Strenkowski JS, Carroll JT (1985). A finite element model of orthogonal metal cutting. ASME J. Eng. Ind., 107: 346–354.
Strenkowski JS, Moon KJ (1990). Finite element prediction of chip geometry and tool/workpiece temperature distributions in orthogonal metal cutting. ASME J. Eng. Ind., 112: 313–318.
Tay AO, Stevenson MG (1974). Using the finite element method to determine temperature distributions in orthogonal machining. Proc. Inst. Mech. Eng., 188: 627–638.
Ueda K, Manabe K (1993). Rigid-plastic FEM analysis of three-dimensional deformations field in the chip formation process. Annals of the CIRP. 42: 35–38.
Usui E, Shirakashi T(1982). Mechanics of machining from descriptive to predictive theory. In on the art of cutting metals-75 years later. ASME Pub. PED. 7: 13–35.
Vignjevic R (2004). Review of development of the Smooth Particle Hydrodynamics (SPH) method. Dynamics and Control of Systems and Structures in Space (DCSSS), 6th conf. Riomaggiore. Italy.
Villumsen M, Fauerholdt T (2008). Simulation of Metal Cutting using Smooth Particle Hydrodynamics. LS-DYNA. Anwenderforum, Bamberg. 17-36.
Wince NJ (2002). Modeling Chip Formation in Orthogonal Metal Cutting using Finite Element Analysis. Msc. Thesis. Mississippi State Univetsity. USA.
Yan H, Hua J, Shivpuri R (2007). Flow stress of AISI H13 die steel in hard machining. Mat. Design, 28(1): 272-277.
Yang X, Liu CR (2002). A new stress-based model of friction behavior in machining and its significant impact on residual stresses computed by finite element method. Int. J. Mech. Sci., 44: 703–723.
Zhang B, Bagchi A (1994). Finite element formation of chip formation and comparison with machining experiment. ASME J. Eng. Ind., 116: 289–297.
Zhang L (1999). On the Separation Criteria in the Simulation of Orthogonal Metal Cutting Using the Finite Element Method. J. Mat. Pro. Technol., 90: 273-278.